The structure of a nucleolytic ribozyme that employs a catalytic metal ion

Liu, Yijin; Wilson, Timothy; Lilley, David

Published in:
Nature Chemical Biology

DOI:
10.1038/nchembio.2333

Publication date:
2017

Document Version
Peer reviewed version

The structure of a nucleolytic ribozyme, with an important role for a catalytic metal ion

Yijin Liu, Timothy J. Wilson and David M.J. Lilley

SUPPLEMENTARY INFORMATION

SUPPLEMENTARY RESULTS

SUPPLEMENTARY FIGURES

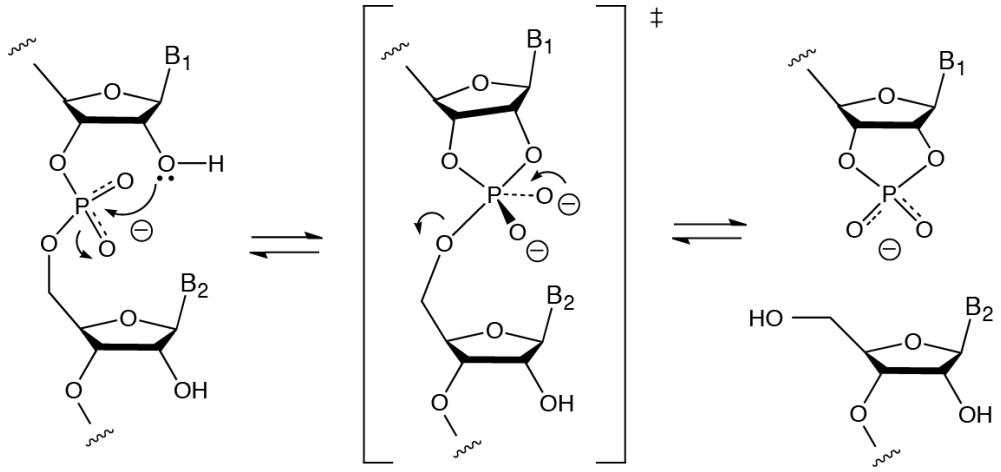

Supplementary Figure 1 The mechanism of cleavage in the nucleolytic ribozymes. The O2' nucleophile attacks the P in an S_N2 reaction, with departure of the O5' leaving group to leave a cyclic 2',3'-phosphate and a 5'-hydroxyl. The transition state of the reaction will be close to the phosphorane structure (center) in which the O2', P and O5' atoms are co-linear.

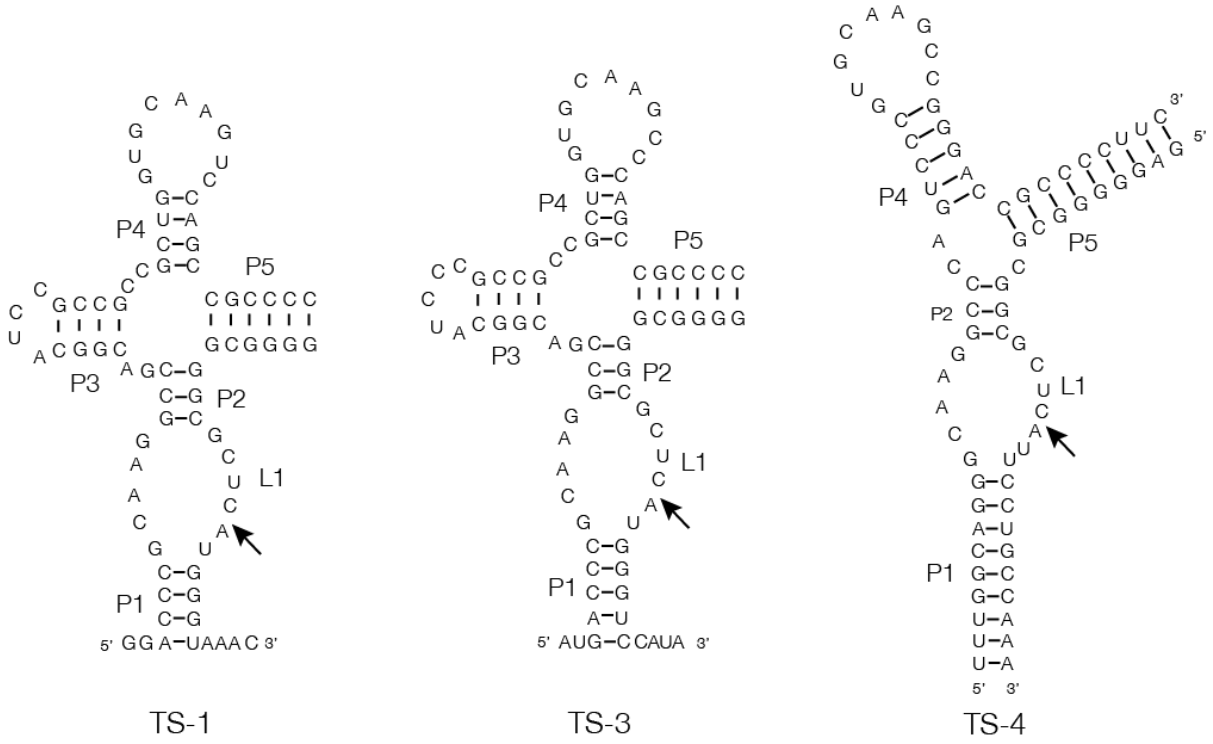

Supplementary Figure 2 Sequence and secondary structures of TS ribozymes studied in the Breaker lab (1).

1. Weinberg, Z., Kim, P.B., Chen, T.H., Li, S., Harris, K.A., Lunse, C.E. and Breaker, R.R. (2015) New classes of self-cleaving ribozymes revealed by comparative genomics analysis. *Nature Chem. Biol.*, **11**, 606-610.

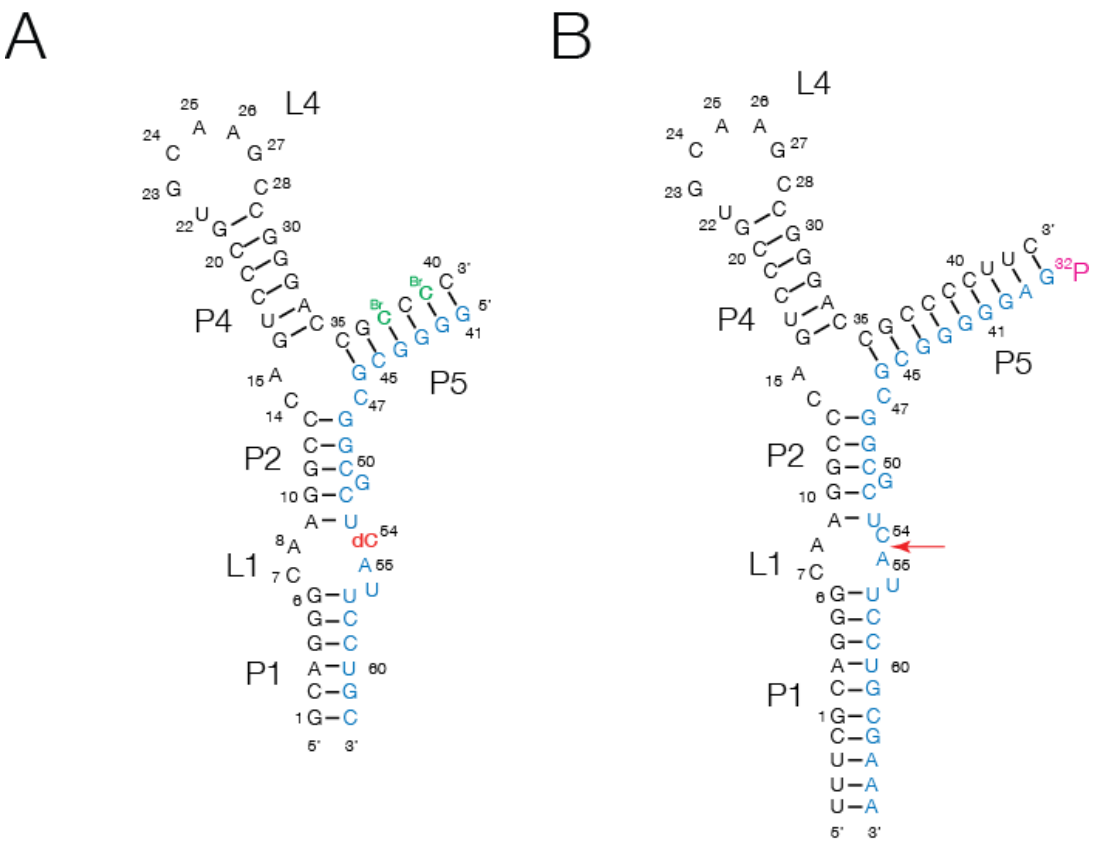

Supplementary Figure 3 Sequences of RNA constructs used in crystallization and studies of ribozyme activity. Both are constructed from two strands, colored black and blue here.

A. The TS construct used for crystallization. The P1 and P5 helices have been shortened in this construct. C54 was replaced by 2'-deoxycytosine (highlighted red) in order to prevent ribozyme cleavage by removal of the nucleophile. C37 and C39 were replaced with 5-bromocytosine (highlighted green) used to provide phase information by SAD.

B. The TS construct used for activity studies. C54 has a normal ribose, and ribozyme cleavage occurs at the position arrowed in red. The substrate strand (blue) is radioactively-[5'^{32}P]-labelled in these experiments. Note that aside from the different lengths of the P1 and P5 helices, the sequence of the ribozyme used in activity studies was identical to that using for crystallography.

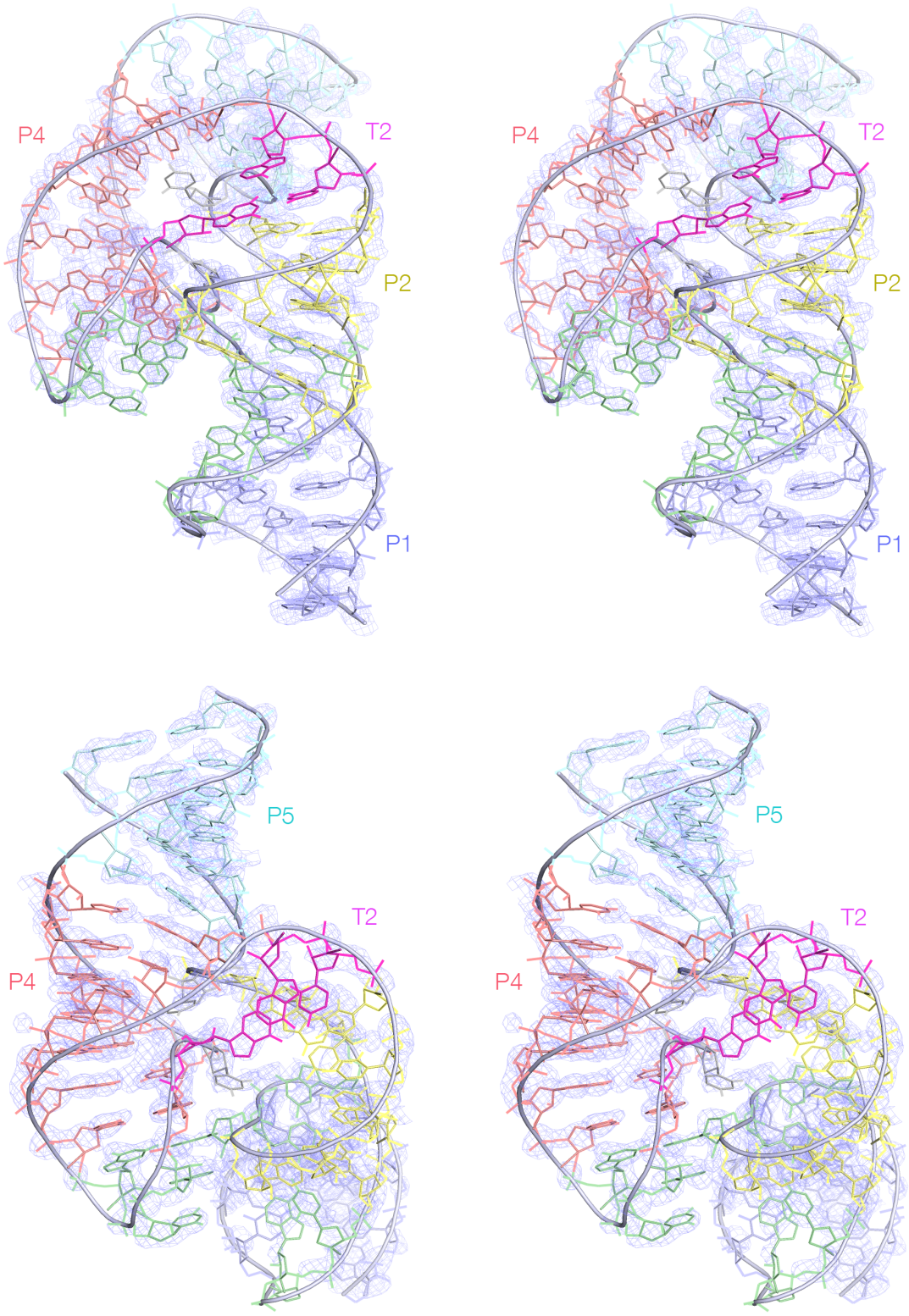

Supplementary Figure 4 Two parallel-eye stereoscopic views of the complete ribozyme showing the experimental SAD phasing electron density map contoured at 1.5σ. In the upper view the axis of the P1-L1-P2-T2 axis is approximately vertical, while in the lower view the P4-P5 axis is approximately vertical. The two axes are inclined at a relative angle of 40°.

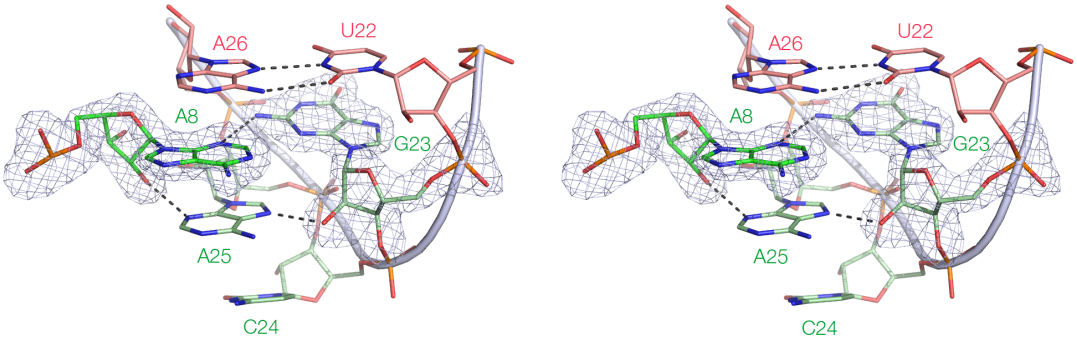

Supplementary Figure 5 Parallel-eye stereoscopic view of the T1 tertiary interaction with the L4 loop, showing the $\mathbf{F}_o$-$\mathbf{F}_c$ omit map contoured at 3σ for A8 and G23.

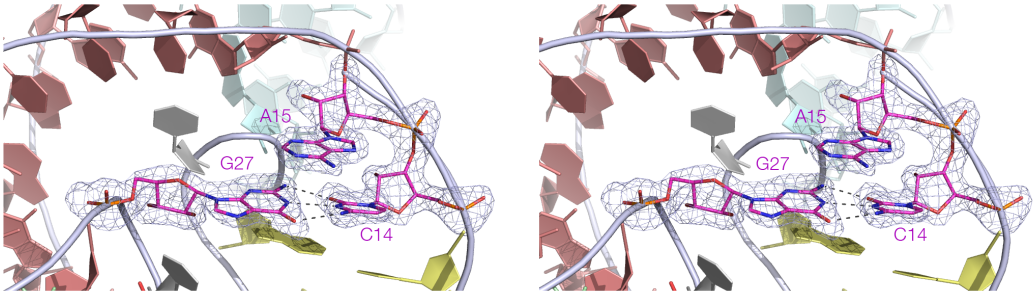

Supplementary Figure 6 Parallel-eye stereoscopic view of the T2 tertiary interaction showing the $\mathbf{F}_o$-$\mathbf{F}_c$ omit map contoured at 3σ for G27, C14 and A15.

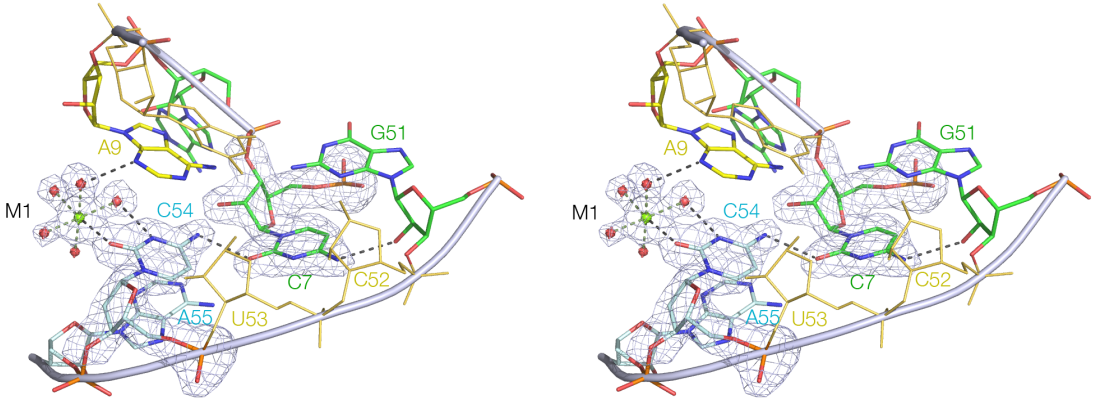

Supplementary Figure 7 Parallel-eye stereoscopic view of the L1 loop and active center of the ribozyme showing the $\mathbf{F}_o$-$\mathbf{F}_c$ omit map contoured at 3σ for C54, C7 and the hydrated metal ion M1 bound to C54. The nucleobases of C52 and U53 have been undisplayed for clarity.

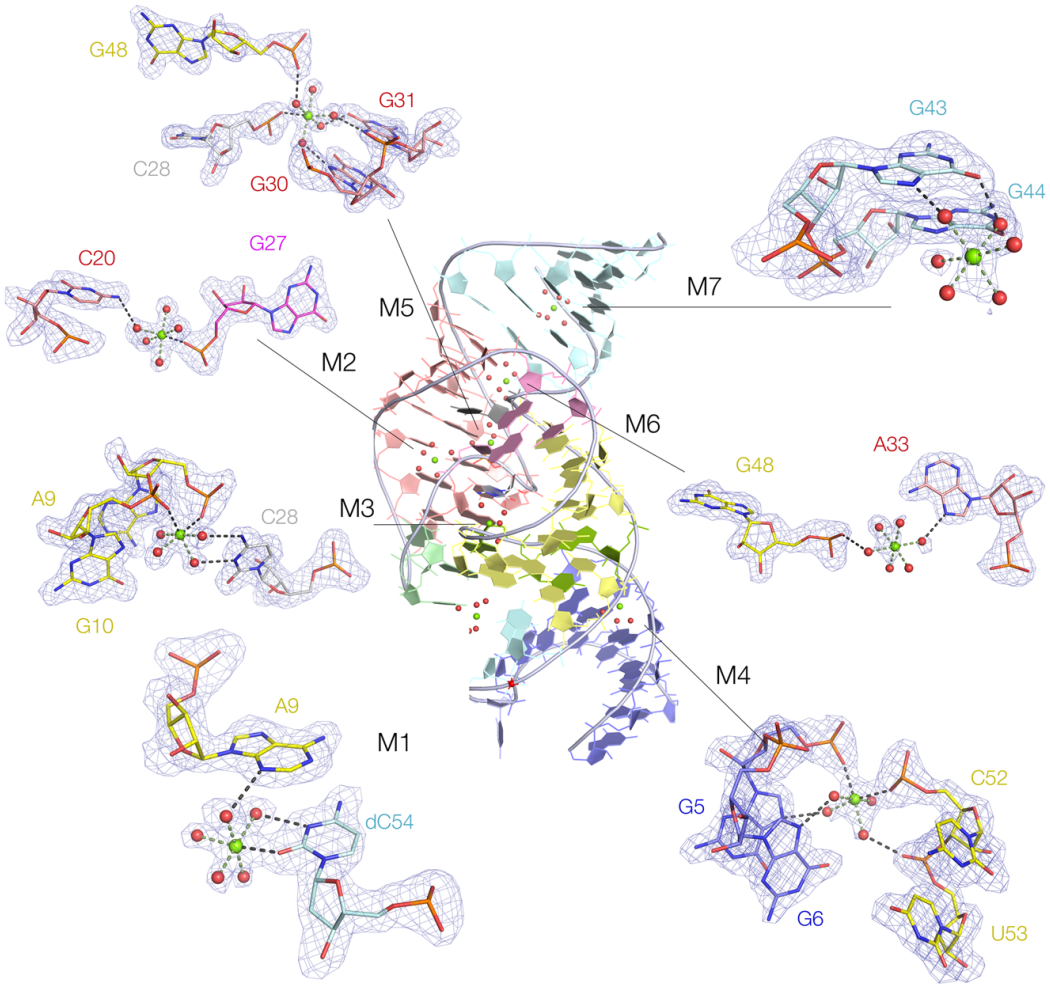

Supplementary Figure 8 Metal ions observed bound to the structure of the TS ribozyme. The local environment of each metal ion is shown in the individual views, with $\mathbf{F}_o$-$\mathbf{F}_c$ omit maps for each contoured at 3σ. M6 and M7 are only partially occupied with less-well defined electron density compared with the other five metal ions.

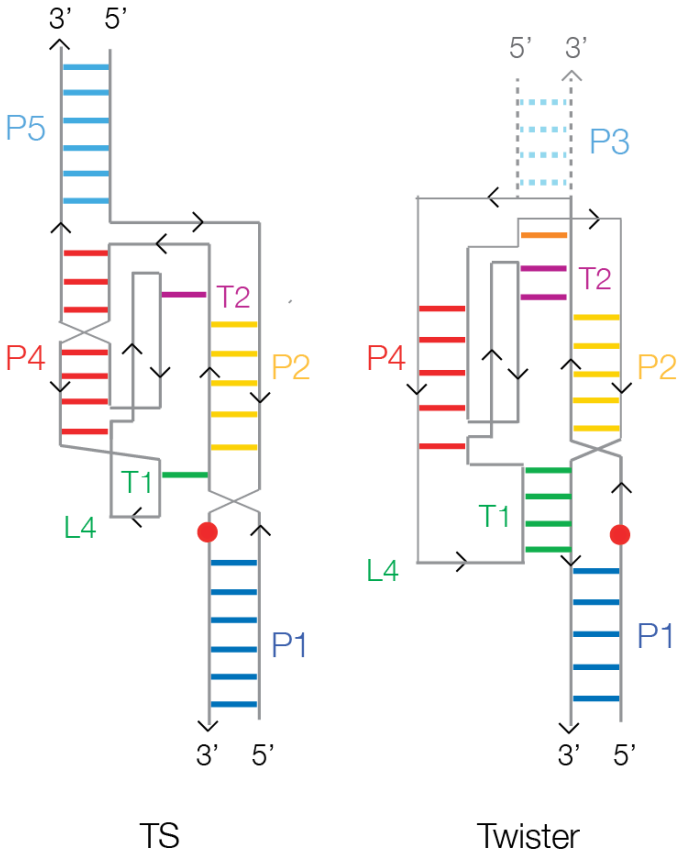

Supplementary Figure 9 Comparison of the topological structures of TS and twister ribozymes. The scissile phosphates in both structures are indicated by the red circles.

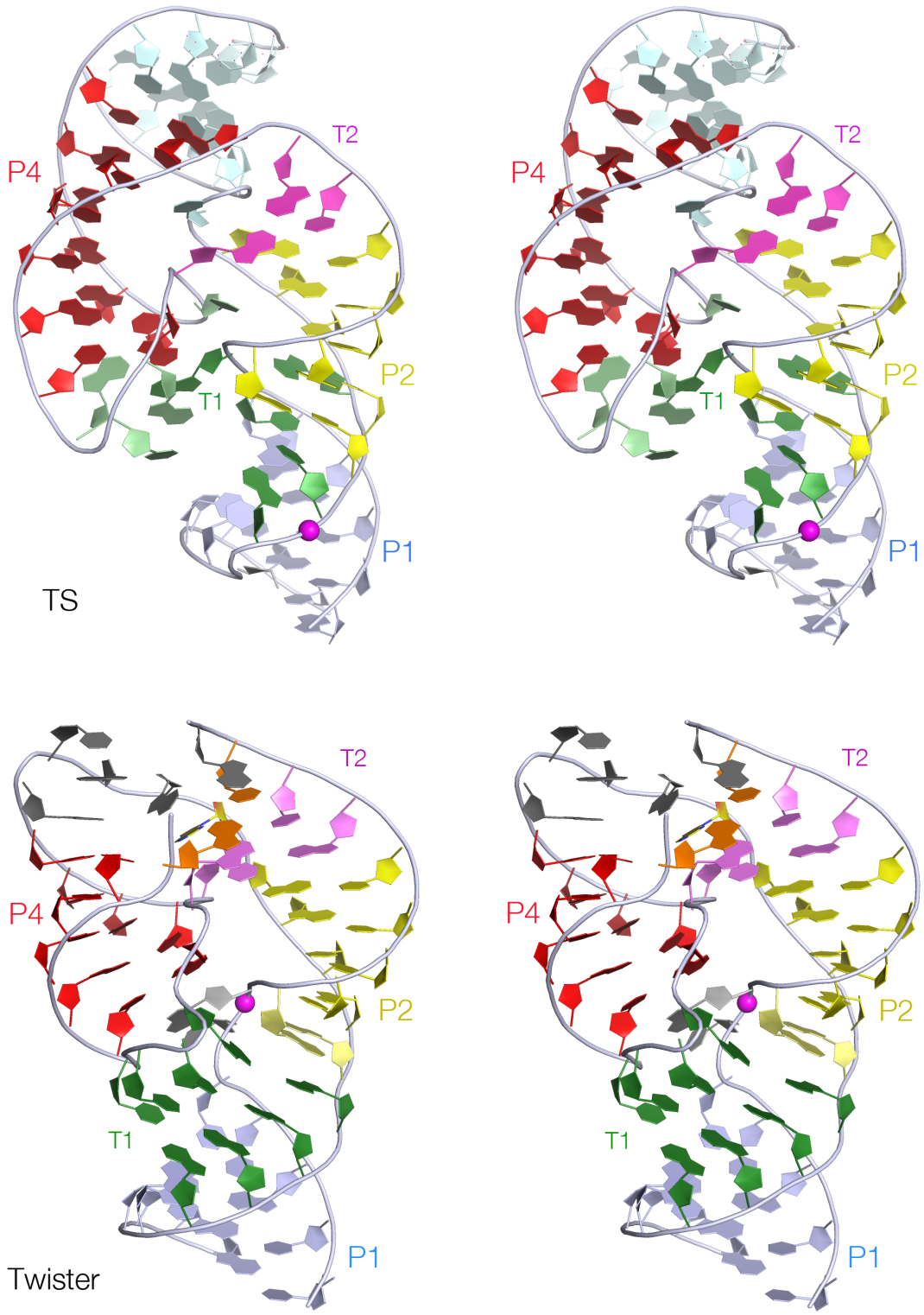

Supplementary Figure 10 Comparison of the crystal structures of TS and twister ribozymes. The scissile phosphates in both structures are indicated by the magenta spheres. To aid comparison the two species have been colored similarly, and shown in equivalent points of view.

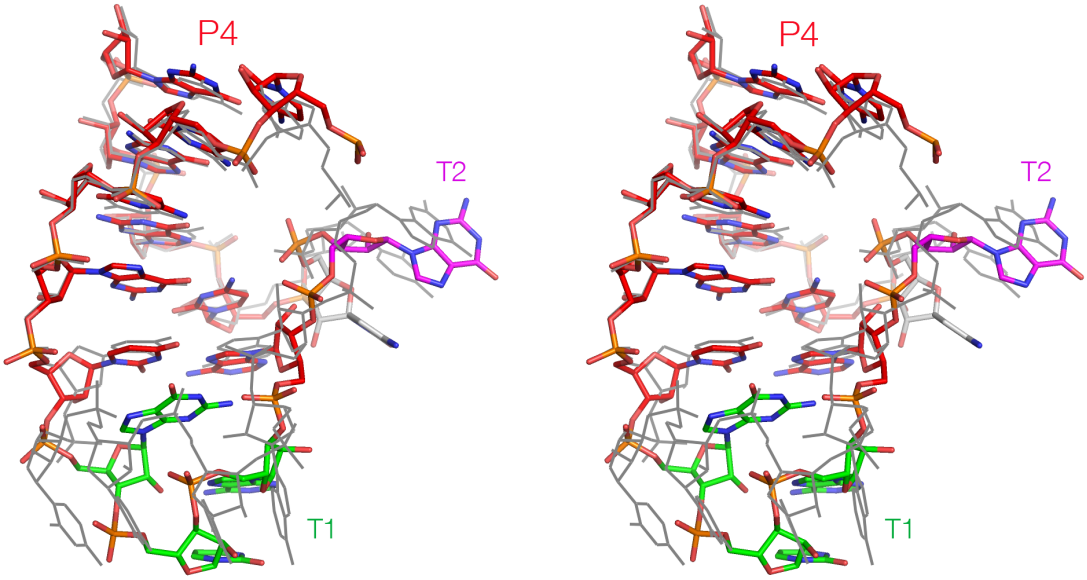

Supplementary Figure 11 Superposition of the P4-L4 regions of TS and twister ribozymes. The TS structure is colored as above, while the twister structure is shown grey. The tertiary elements T1 and T2 in both ribozymes are indicated.

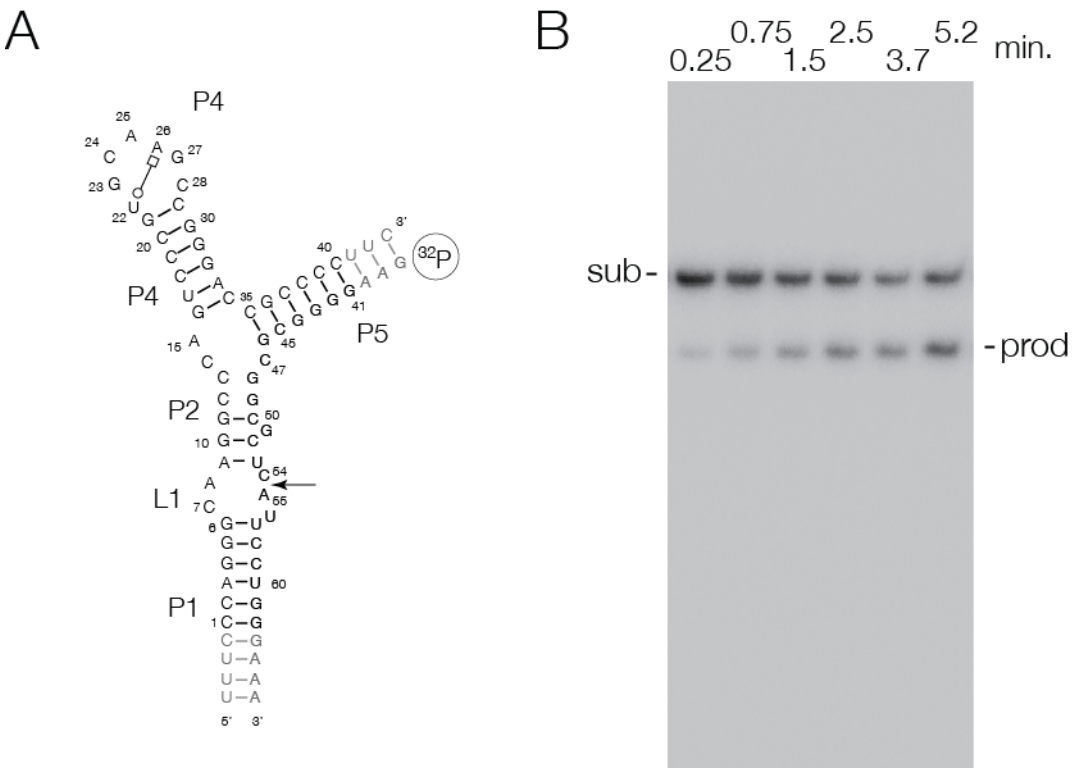

Supplementary Figure 12 The effect of metal ions on cleavage rates by the TS ribozyme.

A. Sequence and 2y structure of the TS-4 construct used to measure rates of cleavage. The position of ribozyme cleavage is arrowed. The substrate strand (black) is radioactively [5'-^{32}P]-labeled.

B. An example of the separation of substrate (sub) and product (prod(by gel electrophoresis at various times (written above each track) in the presence of Mg^{2+} ions.

SUPPLEMENTARY TABLES

Supplementary Table 1

	TS-SAD
Data collection	
Space group	P 4_12_12
Cell dimensions	
a, *b*, *c* (Å)	39.30, 39.30, 228.41
α, β, γ (°)	90.00, 90.00, 90.00
Resolution (Å)	37.16-2.0 (2.07-2.0) *
R_{sym} or R_{merge}	0.07359 (0.3758)
I / σI	28.95 (5.83)
Completeness (%)	97 (80)
Redundancy	21.1 (11.8)
CC1/2	0.999 (0.956)
Refinement	
Resolution (Å)	37.16-2.0 (2.07-2.0)
No. reflections	12723 (1014)
R_{work} / R_{free}	0.1726 / 0.2197
No. atoms	
RNA	1320
Ligand/ion	7
Water	100
B-factors	
RNA	30.34
Ligand/ion	32.82
Water	31.33
R.m.s. deviations	
Bond lengths (Å)	0.008
Bond angles (°)	1.34

Supplementary Table 1 Details of data collection and refinement statistics for the data as deposited in the PDB. Statistics for the highest resolution shell are in parenthesis.

Supplementary Table 2

ion	ligands H_2O	RNA	water - RNA H-bonds	location and role
M1	5	C54 O2 2.3Å	C54 N3 2.7 Å A9 N3 2.8 Å	bound at active site
M2	5	G27 *pro*R 2.2 Å	C20 N4 3.1 Å G21 O6 2.6 Å C28 *pro*R 2.8 Å	bridges P4 major groove
M3	4	G10 *pro*R 2.2 Å A9 *pro*R 2.2 Å	C28 N3 2.8 Å C28 N4 2.9 Å G10 N7 2.6 Å	bound in P2 / L1 major groove links to C28 T2 connector
M4	4	G5 *pro*R 2.3 Å C52 *pro*R 2.3 Å	G4 *pro*R 3.1 Å G5 N7 2.8 Å G6 N7 2.7 Å G6 O6 2.8 Å G51 O2' 3.0 Å U53 *pro*R 2.6 Å	bound in very narrow P1 major groove bridging to L1/P2
M5	5	C28 *pro*S 2.3 Å	G30 N7 2.7 Å G31 O6 2.6 Å G31 N7 2.8 Å G48 *pro*R 2.6 Å	bound in turn deep in P4 major groove bridges T2 turn
M6	6		A33 N7 2.8 Å G48 *pro*S 2.8 Å	bound in P4 major groove linked to P2-P5 S-turn
M7	6		G43 N7 2.4 Å G43 O6 2.4 Å G44 N7 2.7 Å G44 O6 2.8 Å	bound in P5 major groove

Supplementary Table 2. Metal ions observed bound to the TS ribozyme. All water-metal distances were either 2.2 or 2.1 Å with an average of 2.18 Å. Each metal has six inner-sphere ligands with octahedral symmetry. See also Figure S7. M6 and M7 are only partially occupied with significantly less-well defined electron density compared with the other metal ions. It indicates these two metal ion may not play an important role in stabilizing the RNA molecule.

Supplementary Table 3

ribozyme	rate / min^{-1}	standard deviation	fold reduction
TS4	1.78	0.31	
C7 5F	0.0019	0.0012	940
C7 U	< $1x10^{-5}$		
C7 Z	< $1x10^{-5}$		
A9 O2'H	0.55	0.20	3.2
A9 N3CH O2'H	0.0020	0.0011	890
G23 2AP	1.00	0.35	1.8
C24 Z	1.44	0.42	1.2
A25 inosine	0.51	0.16	3.5
A25 purine	0.85	0.15	2.1
A25 N7CH	0.091	0.021	20
G51 O2'H	0.00108	0.00043	1600
C54 U	1.51	0.62	1.2
A55 O2'H	0.187	0.008	9.5
A55 N3CH O2'H	0.0065	0.0017	270
ΔU56	0.96	0.32	1.9
1 M LiCl	$5.7x10^{-5}$	$2.4x10^{-5}$	31000
1 mM $Co(NH_3)_6Cl_3$	< $1x10^{-5}$		
0.2 mM $MnCl_2$	13	2.0	0.14
0.2 mM $CaCl_2$	0.066	0.010	27
0.2 mM $SrCl_2$	0.0025	0.0014	710

Supplementary Table 3. Rates of cleavage by the TS ribozyme as a function of sequence and metal ion composition. All rates measured in 30 mM HEPES (pH 7.0), 100 mM KCl at 25°C, in the presence of 0.2 mM $MgCl_2$ except where indicated. Z = zebularine, 2AP = 2-aminopurine. The data reported are the mean and standard deviation of at least three independent experiments.